

Distributed Robust Artificial-Noise-Aided Secure Precoding for Wiretap MIMO Interference Channels

Zhengmin Kong, *Senior Member, IEEE*, Jing Song, Shaoshi Yang, *Senior Member, IEEE*, Li Gan, Weizhi Meng, *Senior Member, IEEE*, Tao Huang, *Senior Member, IEEE*, and Sheng Chen, *Life Fellow, IEEE*

Abstract—We propose a distributed artificial noise-assisted precoding scheme for secure communications over wiretap multi-input multi-output (MIMO) interference channels, where K legitimate transmitter-receiver pairs communicate in the presence of a sophisticated eavesdropper having more receive-antennas than the legitimate user. Realistic constraints are considered by imposing statistical error bounds for the channel state information of both the eavesdropping and interference channels. Based on the asynchronous distributed pricing model, the proposed scheme maximizes the total utility of all the users, where each user's utility function is defined as the secrecy rate minus the interference cost imposed on other users. Using the weighted minimum mean square error, Schur complement and sign-definiteness techniques, the original non-concave optimization problem is approximated with high accuracy as a quasi-concave problem, which can be solved by the alternating convex search method. Simulation results consolidate our theoretical analysis and show that the proposed scheme outperforms the artificial noise-assisted interference alignment and minimum total mean-square error-based schemes.

Index Terms—Physical layer security, robust optimization, artificial noise, distributed precoding, MIMO, interference channel

I. INTRODUCTION

SECURE communications in information-theoretic interference channel (IC) are vital for numerous applications, e.g., massive device-to-device communications and Internet-of-Things in the 5G and 6G era [1]. This fact requires the study of physical layer security (PLS) to evolve from the simplified scenario that relies on point-to-point channel to the

realistic scenario that depends on the complex IC [2]–[10]. However, the broadcast nature of wireless communication leads to challenging interference management issues when multiuser communications characterized by the IC model are considered [11].

Interference alignment (IA), which can achieve the optimal degrees of freedom for various interference-limited networks under certain conditions [12], [13], is regarded as a promising approach to interference management in IC. For each receiver of the traditional IA scheme, the interferences imposed by multiple individual transmitters are aligned through cooperative precoding into the same interference subspace, which is orthogonal to the signal subspace. Then, the desired signal can be recovered at each receiver as in an interference-free environment [14]. However, there exist a variety of significant challenges for the practical utilization of IA, such as the overhead for obtaining the global channel state information (CSI) [15] and the threat caused by a sophisticated multi-antenna eavesdropper (Eve)¹.

To reduce the overhead of acquiring the global CSI, Abrardo et al. [4] formulated a distributed weighted secrecy rate maximization problem that jointly optimizes the minimum mean-square error (MMSE) based precoder and the successive interference cancellation (SIC) based receiver in multi-input multi-output IC (MIMO-IC)². By considering the sophisticated multi-antenna Eve, the joint design of transmitter precoding matrix and receiver filtering matrix based on IA was developed in [5] for secure communication over wiretap MIMO-IC under the minimum total mean-square error (MT-MSE) criterion. However, the authors of [5] approached the MT-MSE based problem as a non-cooperative game, in which each user selfishly maximizes their utilities in a distributed fashion, regardless of its interference imposed on other users. Thus, its equilibrium may not maximize the sum secrecy rate. Moreover, perfect CSI was assumed, which is extremely difficult to achieve in a practical MIMO-IC. Considering imperfect CSI of the eavesdropping channel (EC), Zhao et al. [6] proposed an artificial noise (AN) assisted IA (AN-IA) scheme to interrupt the external passive Eve, where the accurate CSI of IC is required to eliminate the inter-user interference (IUI) and the ANs imposed by other transmitters on the individual receivers. Furthermore, assuming imperfect CSI of both IC and EC,

Corresponding author: Shaoshi Yang.

This work was supported in part by National Natural Science Foundation of China (No. 62173256), in part by National Key R&D Program of China (No. 2021ZD0112702), and in part by Beijing Municipal Natural Science Foundation (No. L242013).

Z. Kong and L. Gan are with the Department of Artificial Intelligence and Automation, School of Electrical Engineering and Automation, Wuhan University, Wuhan 430072, China (e-mails: zmkong@whu.edu.cn, ligan@whu.edu.cn).

J. Song is with Kunming Power Supply Bureau, Yunnan Power Grid Co., Ltd., Kunming 650000, China (e-mail: songjing@km.yn.csg.cn).

S. Yang is with the School of Information and Communication Engineering, Beijing University of Posts and Telecommunications, with the Key Laboratory of Universal Wireless Communications, Ministry of Education, and also with the Key Laboratory of Mathematics and Information Networks, Ministry of Education, Beijing 100876, China (e-mail: shaoshi.yang@bupt.edu.cn).

Weizhi Meng is with the School of Computing and Communications, Lancaster University, Lancaster LA1 4YW, U.K., and also with the Department of Applied Mathematics and Computer Science, Technical University of Denmark, 2800 Kongens Lyngby, Denmark (e-mail: w.meng3@lancaster.ac.uk).

Tao Huang is with the College of Science and Engineering, James Cook University, Smithfield Cairns, QLD 4878, Australia (e-mail: tao.huang1@jcu.edu.au).

Sheng Chen is with the School of Electronics and Computer Science, University of Southampton, Southampton SO17 1BJ, U.K. (e-mail: sqc@ecs.soton.ac.uk).

¹A sophisticated multi-antenna Eve is an eavesdropper with a sufficient number of antennas, who is capable of eliminating the interferences from other users in the MIMO-IC network and therefore can successfully eavesdrop on the target user.

²The MIMO-IC is composed of multiple transmitter-receiver pairs communicating in parallel, where each node is equipped with multiple antennas and each transmitter imposes interference on its unintended receivers.

robust coordinated beamforming (CB) and power split scheme were studied in [7] for maximizing the sum secrecy rate over the multi-input single-output IC (MISO-IC). In [8], an asynchronous distributed pricing (ADP) algorithm was presented for distributed cooperative power allocation in the single-input single-output IC (SISO-IC). In addition, the work [16] analyzed the secrecy performance of a RIS-assisted multiuser massive MIMO system with AN and realistic constraints, including RIS phase noise and imperfect CSI. The authors of [17] investigated PLS for the RIS-assisted integrated sensing and communication systems, aiming to maximize the achievable sum secrecy rate by jointly optimizing the active and passive beamforming vectors. To the best of our knowledge, the existing contributions fail to ensure secure communications in the challenging distributed cooperative MIMO-IC when facing a sophisticated multi-antenna Eve and imperfect CSI. It is worth emphasizing that the perfect CSI of both the EC and IC is typically unavailable at each transmitter.

Against the above backdrop, we propose a distributed robust AN-aided secrecy precoding scheme based on imperfect CSI for wiretap MIMO-IC. Motivated by [8], to improve the equilibrium efficiency in the distributed cooperative MIMO-IC, we design an ADP mechanism, which is proved to satisfy the Karush-Kuhn-Tucker (KKT) conditions of the global sum secrecy rate maximization problem. Different from [8], however, in the case of imperfect CSI, the robust utility maximization problem for optimizing AN-aided secrecy precoding becomes intractable due to the non-concave objective function, the non-convex constraints, and the channel uncertainties. Facing the above challenges, we first transform the non-concave objective function into a quasi-concave one by employing the weighted MMSE (WMMSE) method [18]. Then, the Schur complement [19] and sign-definiteness [20] techniques are utilized to decouple the imperfect CSI constraints and transform these non-convex constraints into the linear matrix inequality (LMI) constraints. As a result, an approximate solution with high accuracy can be found by the alternating convex search (ACS) method [21]. Numerical results demonstrate the efficiency of the proposed scheme under imperfect CSI. For better clarity, a comparison of the main features of our proposed scheme with those of the existing works is presented in Table I.

The rest of this paper is organized as follows. In Section II, we describe the system model and formulate the correspond-

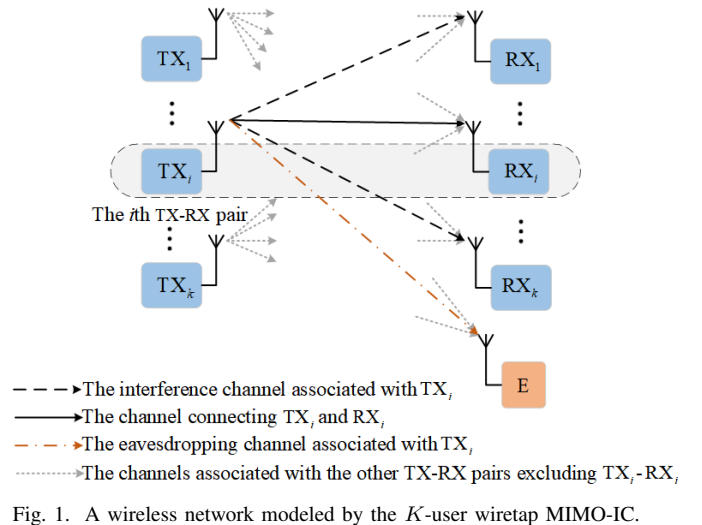


Fig. 1. A wireless network modeled by the K -user wiretap MIMO-IC.

ing optimization problem. Section III proposes a distributed artificial noise-assisted precoding scheme for secure communications using the ADP model. We also characterize both the convergence and the complexity of our scheme. Numerical results are provided in Section IV to evaluate the performance of the proposed algorithm. Finally, our conclusions are drawn in Section V.

Notation: $(\cdot)^T$, $(\cdot)^H$, and $(\cdot)^*$ denote the transpose, conjugate transpose, and optimal solution, respectively. $\text{vec}(\cdot)$, $\text{rank}(\cdot)$, $\text{det}(\cdot)$, $\text{tr}(\cdot)$, and $\|\cdot\|_F$ represent the vectorization, rank, determinant, trace, and Frobenius norm of a matrix, respectively. $\ln(\cdot)$ denotes the natural logarithm, and \otimes represents the Kronecker product.

II. SYSTEM MODEL AND PROBLEM FORMULATION

Consider a wireless network characterized by the K -user wiretap MIMO-IC model, as shown in Fig. 1. Each N_T -antenna transmitter ($TX_i, i \in \{1, \dots, K\}$) intends to send confidential messages to its corresponding N_R -antenna receiver (RX_i) in the presence of a sophisticated Eve (E) having N_E antennas, where $N_E > N_R$. In addition to receiving confidential messages from the corresponding transmitter TX_i , the receiver RX_i also receives interference from the other transmitters TX_j ($j \neq i$). The sophisticated multi-antenna Eve E intends to eavesdrop on a particular transmitter, e.g., TX_i .

TABLE I
COMPARISON OF OUR PROPOSED SCHEME AGAINST THE EXISTING CONTRIBUTIONS

Feature Scheme	MIMO-IC	distributed processing	cooperative game	Eve	Imperfect CSI of EC	Imperfect CSI of IC
Our proposed scheme	✓	✓	✓	✓	✓	✓
IA [3]	✓					
MMSE-SIC [4]	✓	✓				
MT-MSE [5]	✓	✓		✓		
AN-IA [6]	✓			✓	✓	
CB [7]				✓	✓	✓
ADP [8]		✓	✓			

Since $N_E > N_R$, Eve is more powerful than any legitimate receiver of the network in terms of the spatial-domain signal processing capability. Therefore, even if the legitimate receiver RX_i cannot decode the message sent by its corresponding transmitter TX_i , it is still possible for E to eliminate the interference generated by the other transmitters TX_j and decode the signal from the transmitter TX_i of interest. Our AN-aided secrecy precoding scheme aims to prevent eavesdropping and reduce the IUI imposed on legitimate receivers.

Let user i be the desired user considered. The signal transmitted by TX_i can be written as

$$\mathbf{x}_i = \mathbf{Q}_i \mathbf{s}_i + \mathbf{\Lambda}_i \mathbf{z}_i, \quad (1)$$

where $\mathbf{s}_i \in \mathbb{C}^{d_s \times 1}$ and $\mathbf{z}_i \in \mathbb{C}^{d_a \times 1}$ denote the confidential-message bearing signal and the AN, respectively, $\mathbf{Q}_i \in \mathbb{C}^{N_T \times d_s}$ is the secrecy precoding matrix for \mathbf{s}_i , and $\mathbf{\Lambda}_i \in \mathbb{C}^{N_T \times d_a}$ is the AN precoding matrix for \mathbf{z}_i . Each transmitted signal must satisfy the following power constraint:

$$\text{tr}(\mathbf{Q}_i \mathbf{Q}_i^H + \mathbf{\Lambda}_i \mathbf{\Lambda}_i^H) \leq P_{\text{tot}}, \quad (2)$$

where P_{tot} is the total available power of each transmitter. In a scheduling time slot, the signal received at RX_i can be expressed as

$$\mathbf{y}_i = \sqrt{\omega_M} \bar{\mathbf{H}}_{i,i} \mathbf{x}_i + \sum_{j \neq i} \sqrt{\omega_I} \bar{\mathbf{H}}_{i,j} \mathbf{x}_j + \mathbf{n}_i, \quad (3)$$

where $\bar{\mathbf{H}}_{i,i} \in \mathbb{C}^{N_R \times N_T}$ is the true small-scale Rayleigh fading CSI of the (main) channel from TX_i to RX_i , $\bar{\mathbf{H}}_{i,j} \in \mathbb{C}^{N_R \times N_T}$ is the true small-scale Rayleigh fading CSI of the IC from TX_j to RX_i , and $\mathbf{n}_i \in \mathbb{C}^{N_R \times 1}$ is the additive white Gaussian noise (AWGN) vector with zero mean and covariance matrix $\sigma_{R_i}^2 \mathbf{I}$ [22]. Entries of $\bar{\mathbf{H}}_{i,i}$ and $\bar{\mathbf{H}}_{i,j}$ are independent and identically distributed (i.i.d) complex Gaussian random variables following the distribution $\mathcal{CN}(0, 1)$. Also $\omega_M = \kappa d_M^{-\tau}$ and $\omega_I = \kappa d_I^{-\tau}$ are the large-scale path-loss coefficients of the main channel and IC, respectively, where $\tau = 2.6$ is the path-loss exponent and $\kappa = 10^{-4}$ is the path-loss at unit distance [23], while d_M and d_I are the distances between transmitters and receivers of the main channel and IC, respectively.

In practice, we usually do not know about Eve. Hence, we assume the worst-case scenario where the sophisticated multi-antenna Eve can eliminate the interference imposed on its target user, i.e., user i . Therefore, when E wiretaps on user i , the signal received at the Eve is written as

$$\mathbf{y}_{E_i} = \sqrt{\omega_E} \bar{\mathbf{H}}_{E_i} \mathbf{x}_i + \mathbf{n}_{E_i}, \quad (4)$$

where $\bar{\mathbf{H}}_{E_i} \in \mathbb{C}^{N_E \times N_T}$ is the true small-scale Rayleigh fading CSI of the EC from TX_i to E, whose entries are i.i.d complex Gaussian random variables following $\mathcal{CN}(0, 1)$, and $\omega_E = \kappa d_E^{-\tau}$ is the large-scale path-loss coefficient of the EC with d_E denoting the distance between TX_i and E, while $\mathbf{n}_{E_i} \in \mathbb{C}^{N_E \times 1}$ is the AWGN vector with zero mean and covariance matrix $\sigma_{E_i}^2 \mathbf{I}$.

Given the perfect CSI, the real achievable rates of the legitimate user i and of the Eve for the i th TX-RX pair are

respectively given by

$$\bar{C}_{R_i} = \log \det (\mathbf{I} + \bar{\mathbf{Z}}_{R_i} \bar{\mathbf{N}}_{R_i}^{-1}), \quad (5)$$

$$\bar{C}_{E_i} = \log \det (\mathbf{I} + \bar{\mathbf{Z}}_{E_i} \bar{\mathbf{N}}_{E_i}^{-1}), \quad (6)$$

where

$$\bar{\mathbf{Z}}_{R_i} = \omega_M \bar{\mathbf{H}}_{i,i} \mathbf{Q}_i \mathbf{Q}_i^H \bar{\mathbf{H}}_{i,i}^H, \quad (7)$$

$$\bar{\mathbf{N}}_{R_i} = \omega_M \bar{\mathbf{H}}_{i,i} \mathbf{\Lambda}_i \mathbf{\Lambda}_i^H \bar{\mathbf{H}}_{i,i}^H + \sigma_{R_i}^2 \mathbf{I} + \bar{\mathbf{Y}}_i, \quad (8)$$

$$\bar{\mathbf{Z}}_{E_i} = \omega_E \bar{\mathbf{H}}_{E_i} \mathbf{Q}_i \mathbf{Q}_i^H \bar{\mathbf{H}}_{E_i}^H, \quad (9)$$

$$\bar{\mathbf{N}}_{E_i} = \omega_E \bar{\mathbf{H}}_{E_i} \mathbf{\Lambda}_i \mathbf{\Lambda}_i^H \bar{\mathbf{H}}_{E_i}^H + \sigma_{E_i}^2 \mathbf{I}, \quad (10)$$

$$\bar{\mathbf{Y}}_i = \sum_{j \neq i} \omega_I \bar{\mathbf{H}}_{i,j} (\mathbf{Q}_j \mathbf{Q}_j^H + \mathbf{\Lambda}_j \mathbf{\Lambda}_j^H) \bar{\mathbf{H}}_{i,j}^H. \quad (11)$$

Thus, the infimum of the real achievable secrecy rate of the i th TX-RX pair can be written as

$$\begin{aligned} \bar{C}_{S_i} &= \bar{C}_{R_i} - \bar{C}_{E_i} \\ &= \log \det (\mathbf{I} + \bar{\mathbf{Z}}_{R_i} \bar{\mathbf{N}}_{R_i}^{-1}) - \log \det \left(\frac{\bar{\mathbf{N}}_{E_i} + \bar{\mathbf{Z}}_{E_i}}{\bar{\mathbf{N}}_{E_i}} \right) \\ &= \log \det (\mathbf{I} + \bar{\mathbf{Z}}_{R_i} \bar{\mathbf{N}}_{R_i}^{-1}) - \left(\log \det (\bar{\mathbf{N}}_{E_i} + \bar{\mathbf{Z}}_{E_i}) \right. \\ &\quad \left. - \log \det (\bar{\mathbf{N}}_{E_i}) \right). \end{aligned} \quad (12)$$

Under the deterministic model for characterizing the CSI uncertainty [24], we assume that the estimated channel \mathbf{H} lies in the spherical zone centered at the true channel $\bar{\mathbf{H}}$, namely,

$$\mathbf{H} = \bar{\mathbf{H}} + \Delta \mathbf{H}, \quad (13)$$

where $\bar{\mathbf{H}}$ and $\Delta \mathbf{H}$ are independent of each other and their entries are i.i.d complex Gaussian random variables with zero mean and variances of $1 - \zeta^2$ and ζ^2 , respectively, with $\zeta^2 \in [0, 1]$. When the CSI is perfectly known at the transmitter, $\zeta^2 = 0$, while $\zeta^2 = 1$ if the transmitter does not know the CSI [25]. E is assumed to be purely passive; hence, the CSI of wiretap channels is unavailable to the legitimate node. Thus, we adopt uncertainty model [26], which gives

$$\mathbf{H}_{E_i} \in \mathbb{S}_E \triangleq \{\mathbf{H}_{E_i} = \bar{\mathbf{H}}_{E_i} + \Delta \mathbf{H}_{E_i}, \Delta \mathbf{H}_{E_i} \sim \mathcal{CN}(0, \zeta_{E_i}^2 \mathbf{I})\}, \quad (14)$$

$$\mathbf{H}_{i,j} \in \mathbb{S}_R \triangleq \{\mathbf{H}_{i,j} = \bar{\mathbf{H}}_{i,j} + \Delta \mathbf{H}_{i,j}, \Delta \mathbf{H}_{i,j} \sim \mathcal{CN}(0, \zeta_{R_{i,j}}^2 \mathbf{I})\}. \quad (15)$$

Due to the uncertainty in the CSI model, an accurate real channel $\bar{\mathbf{H}}_{E_i}$ and $\bar{\mathbf{H}}_{i,j}$ cannot be obtained. Instead, it is only known that the estimated channel \mathbf{H}_{E_i} and $\mathbf{H}_{i,j}$ lie within the spherical zone centered at the true channel. Consequently, the real achievable secrecy rate cannot be determined, and the estimated achievable secrecy rate of the i th TX-RX pair can be written as

$$\begin{aligned} C_{S_i} &= C_{R_i} - C_{E_i} \\ &= \log \det (\mathbf{I} + \mathbf{Z}_{R_i} \mathbf{N}_{R_i}^{-1}) - \left(\log \det (\mathbf{N}_{E_i} + \mathbf{Z}_{E_i}) \right. \\ &\quad \left. - \log \det (\mathbf{N}_{E_i}) \right), \end{aligned} \quad (16)$$

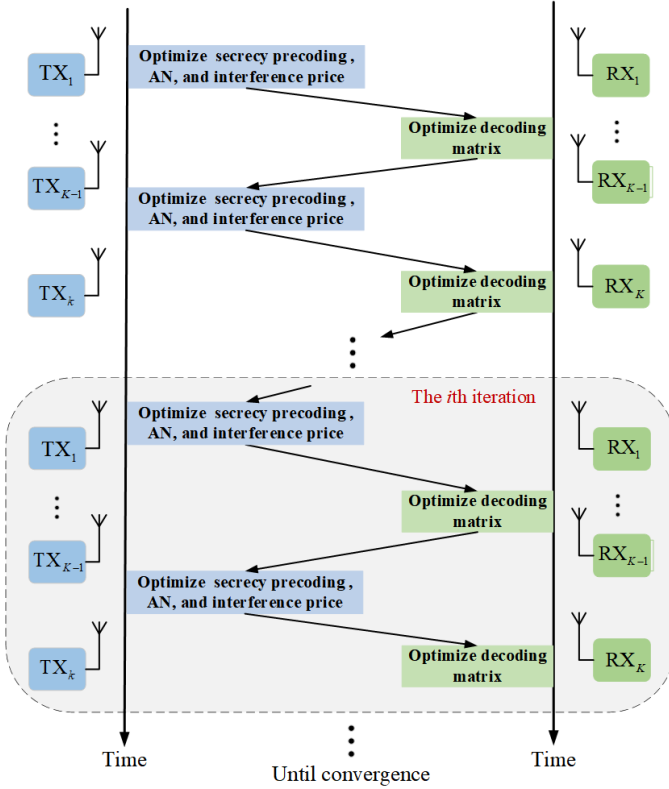


Fig. 2. Distributed ADP model for robust AN-aided secure precoding, where

$$\mathbf{Z}_{R_i} = \omega_M \mathbf{H}_{i,i} \mathbf{Q}_i \mathbf{Q}_i^H \mathbf{H}_{i,i}^H, \quad (17)$$

$$\mathbf{N}_{R_i} = \omega_M \mathbf{H}_{i,i} \mathbf{\Lambda}_i \mathbf{\Lambda}_i^H \mathbf{H}_{i,i}^H + \sigma_{R_i}^2 \mathbf{I} + \mathbf{\Upsilon}_i, \quad (18)$$

$$\mathbf{Z}_{E_i} = \omega_E \mathbf{H}_{E_i} \mathbf{Q}_i \mathbf{Q}_i^H \mathbf{H}_{E_i}^H, \quad (19)$$

$$\mathbf{N}_{E_i} = \omega_E \mathbf{H}_{E_i} \mathbf{\Lambda}_i \mathbf{\Lambda}_i^H \mathbf{H}_{E_i}^H + \sigma_{E_i}^2 \mathbf{I}, \quad (20)$$

$$\mathbf{\Upsilon}_i = \sum_{j \neq i} \omega_j \mathbf{H}_{i,j} (\mathbf{Q}_j \mathbf{Q}_j^H + \mathbf{\Lambda}_j \mathbf{\Lambda}_j^H) \mathbf{H}_{i,j}^H. \quad (21)$$

Therefore, the transmitters are aware of imperfect CSIs for all receivers, and the *centralized* sum secrecy rate maximization problem for the whole system can be formulated as

$$\mathcal{P}_1 : \max_{\mathbf{Q}_i \geq \mathbf{0}, \mathbf{\Lambda}_i \geq \mathbf{0}} \sum_{i=1}^K C_{S_i}, \quad (22a)$$

$$\text{s.t. } \text{tr}(\mathbf{Q}_i \mathbf{Q}_i^H + \mathbf{\Lambda}_i \mathbf{\Lambda}_i^H) \leq P_{\text{tot}}, \quad (22b)$$

$$\forall \mathbf{H}_{i,j} \in \mathbb{S}_R, \forall \mathbf{H}_{E_i} \in \mathbb{S}_E, i, j \in \{1, 2, \dots, K\}. \quad (22c)$$

To calculate $\sum_{i=1}^K C_{S_i}$, a central node that can obtain all CSI $\mathbf{H}_{i,j}, i, j \in \{1, \dots, K\}$ is needed to calculate the secrecy precoding matrix, AN precoding matrix and decoding matrices for each transmitter. Then, the calculated result is transmitted back to each transmitter. To ensure that the central node can obtain the global CSI, each TX_i – RX_i pair needs to send the channel it can obtain (\mathbf{H}_{E_i} and $\mathbf{H}_{i,j}$) to the central node.

III. DISTRIBUTED ROBUST AN-AIDED SECRECY PRECODING EMPLOYING THE ADP MODEL

A. ADP Model for Robust AN-Aided Secure Precoding

Based on the centralized interference management strategy, the authors of [27]–[30] assume a central node can obtain

the global CSI at transmitters. However, it is a challenge to construct such a central node in practice [31]. In this subsection, we present an ADP model for robust AN-aided secure precoding, as shown in Fig. 2. In contrast to the centralized model, where the global CSI must be made available to all the transmitters via the central node, under the ADP model, only the interference prices of individual TX-RX pairs have to be exchanged between the transmitters. More specifically, the i -th TX-RX pair optimizes its secrecy precoding matrix, AN precoding matrix, and decoding matrices based on the utility function and then calculates the interference price for this TX-RX pair and broadcasts it to other TX-RX pairs, while continuously iterating, until the overall utility function converges. Thus, in our scheme, the limited information the transmitters exchange is the interference price, which reflects the marginal change in the utility per unit interference power.

Relying on the following matrix derivative formula:

$$\frac{\partial \log \det(\mathbf{A} + \mathbf{BXC})}{\partial \mathbf{X}} = \left(\mathbf{C}(\mathbf{A} + \mathbf{BXC})^{-1} \mathbf{B} \right), \quad (23)$$

the explicit expression of the interference price for the i th TX-RX pair can be expressed as

$$\mathbf{\Pi}_i = \frac{\partial C_{S_i}}{\partial \mathbf{\Upsilon}_i} = (\mathbf{Z}_{R_i} + \mathbf{N}_{R_i})^{-1} - (\mathbf{N}_{R_i})^{-1}, \quad (24)$$

where $\mathbf{\Upsilon}_i$ is the total interference received by the i th TX-RX pair. Here, $\mathbf{\Pi}_i$ represents the i th TX-RX pair's marginal increase in utility per unit decrease in total interference.

Given the fixed interference prices and AN-aided secrecy precoding matrices from the other TX-RX pairs, the i th TX-RX pair updates its AN-aided precoding matrix by *distributively* solving the following subproblem:

$$\mathcal{P}_2 : \max_{\mathbf{Q}_i \geq \mathbf{0}, \mathbf{\Lambda}_i \geq \mathbf{0}} f_i, \quad (25a)$$

$$\text{s.t. } \text{tr}(\mathbf{Q}_i \mathbf{Q}_i^H + \mathbf{\Lambda}_i \mathbf{\Lambda}_i^H) \leq P_{\text{tot}}, \quad (25b)$$

$$\forall \mathbf{H}_{i,j} \in \mathbb{S}_R, \forall \mathbf{H}_{E_i} \in \mathbb{S}_E. \quad (25c)$$

Since each TX-RX pair's achievable secrecy rate C_{S_i} is determined without considering interference with other TX-RX pairs, when \mathbf{Q}_j and $\mathbf{\Lambda}_j$ are fixed, the i th TX-RX pair will selfishly maximize their own achievable secrecy rate C_{S_i} while causing greater interference with other TX-RX pairs. Thus, we introduce interference prices and view it as a price charged to other TX-RX pairs for generating interference to i th TX-RX pair. The utility function f_i of the i th TX-RX pair is defined as its secrecy rate minus payment to the other TX-RX pairs in the network due to the interference it generates [8], namely,

$$f_i = C_{S_i} - \sum_{j \neq i} \omega_j \text{tr} \left(\mathbf{\Pi}_j \mathbf{H}_{i,j} (\mathbf{Q}_i \mathbf{Q}_i^H + \mathbf{\Lambda}_i \mathbf{\Lambda}_i^H) \mathbf{H}_{i,j}^H \right). \quad (26)$$

Unlike \mathcal{P}_1 , which focuses on optimizing the achievable secrecy sum-rate at the central node, \mathcal{P}_2 focuses on the utility function of the i th TX-RX pair. Our proposed ADP model sequentially optimizes the utility function $f_i, i \in \{1, 2, \dots, K\}$ of each TX-RX pair among K TX-RX pairs until they reach their maximum values. However, it is necessary to ensure that the i th TX-RX pair can obtain the distribution of CSI (\mathbf{H}_{E_i} and $\mathbf{H}_{i,j}$) related to it.

The robust AN-aided secrecy precoding problem \mathcal{P}_2 is difficult to solve directly due to the non-concave term $-\log \det(\cdot)$ with respect to $\{\mathbf{Q}_i, \mathbf{\Lambda}_i\}$ [32], the nonlinear term $\log \det(\cdot)$ and the imperfect CSI constraints (25c). In order to transform \mathcal{P}_2 into a tractable problem, [32, Proposition 1] is invoked to reformulate the non-concave term as follows:

$$-\log \det(\mathbf{Z}_{E_i} + \mathbf{N}_{E_i}) = \max_{\mathbf{S}_{E_i} \succeq \mathbf{0}} \log \det(\mathbf{S}_{E_i}) - \text{tr}(\mathbf{S}_{E_i}(\mathbf{Z}_{E_i} + \mathbf{N}_{E_i})) + N_E, \quad (27)$$

where $\mathbf{S}_{E_i} \in \mathbb{C}^{N_E \times N_E}$ is the auxiliary variable with its optimal solution expressed in the closed form as:

$$\mathbf{S}_{E_i}^* = (\mathbf{Z}_{E_i} + \mathbf{N}_{E_i})^{-1}. \quad (28)$$

To overcome the difficulty imposed by the nonlinearity $\log \det(\cdot)$, the idea of the WMMSE method [18] is employed to transform the achievable rate into its equivalent counterpart by introducing some auxiliary variables as follows:

$$C_{R_i} = \max_{\mathbf{S}_{R_i} \succeq \mathbf{0}} \log \det(\mathbf{S}_{R_i}) - \text{tr}(\mathbf{S}_{R_i} \mathbf{M}_{R_i}) + d_s, \quad (29)$$

$$\log \det(\mathbf{N}_{E_i}) = \max_{\mathbf{S}_{E+i} \succeq \mathbf{0}} \log \det(\mathbf{S}_{E+i}) - \text{tr}(\mathbf{S}_{E+i} \mathbf{M}_{E_i}) + N_E, \quad (30)$$

where \mathbf{M}_{R_i} and \mathbf{M}_{E_i} are the auxiliary mean-square error (MSE) matrices of RX_i and E, respectively, and they are defined as:

$$\mathbf{M}_{R_i} = \left(\sqrt{\omega_M} \mathbf{U}_{R_i}^H \mathbf{H}_{i,i} \mathbf{Q}_i - \mathbf{I} \right) \left(\sqrt{\omega_M} \mathbf{U}_{R_i}^H \mathbf{H}_{i,i} \mathbf{Q}_i - \mathbf{I} \right)^H + \mathbf{U}_{R_i}^H \mathbf{N}_{R_i} \mathbf{U}_{R_i}, \quad (31)$$

$$\mathbf{M}_{E_i} = \left(\sqrt{\omega_E} \mathbf{U}_{E_i}^H \mathbf{H}_{E_i} \mathbf{\Lambda}_i - \mathbf{I} \right) \left(\sqrt{\omega_E} \mathbf{U}_{E_i}^H \mathbf{H}_{E_i} \mathbf{\Lambda}_i - \mathbf{I} \right)^H + \frac{\omega_E}{\sigma_{E_i}^2} \mathbf{U}_{E_i}^H \mathbf{U}_{E_i}, \quad (32)$$

in which $\mathbf{U}_{R_i} \in \mathbb{C}^{N_R \times d_s}$ and $\mathbf{U}_{E_i} \in \mathbb{C}^{N_E \times d_s}$ are the decoding matrices of the well-known linear MMSE receivers for RX_i and E, respectively, and they can be expressed as

$$\mathbf{U}_{R_i} = (\mathbf{N}_{R_i})^{-1} \mathbf{H}_{i,i} \mathbf{Q}_i, \quad (33)$$

$$\mathbf{U}_{E_i} = \sqrt{\frac{\sigma_{E_i}^2}{\omega_E}} \mathbf{H}_{E_i} \mathbf{\Lambda}_i. \quad (34)$$

Similar to \mathbf{S}_{E_i} of (27), \mathbf{S}_{R_i} and \mathbf{S}_{E+i} in (29) and (30) are also auxiliary variables with their optimal solutions given by

$$\mathbf{S}_{R_i}^* = (\mathbf{M}_{R_i})^{-1}, \quad (35)$$

$$\mathbf{S}_{E+i}^* = (\mathbf{M}_{E_i})^{-1}. \quad (36)$$

To decouple the imperfect CSI constraints (25c), the slack variables α_i , β_i , γ_i and $\theta_{i,j}$ are introduced concerning the imperfect CSIs modeled by (14) and (15). With the aforementioned manipulations, we transform \mathcal{P}_2 into

tioned manipulations, we transform \mathcal{P}_2 into

$$\mathcal{P}_3 : \max_{\mathbf{Q}_i \succeq \mathbf{0}, \mathbf{\Lambda}_i \succeq \mathbf{0}} g_i, \quad (37a)$$

$$\text{s.t. } \text{tr}(\mathbf{\Xi}_{R_i}) \leq \alpha_i, \quad (37b)$$

$$\text{tr}(\mathbf{\Xi}_{E+i}) \leq \beta_i, \quad (37c)$$

$$\text{tr}(\mathbf{\Xi}_{E-i}) \leq \gamma_i, \quad (37d)$$

$$\text{tr}(\mathbf{\Xi}_{R_i,j}) \leq \theta_{i,j}, \quad (37e)$$

$$\text{tr}(\mathbf{Q}_i \mathbf{Q}_i^H + \mathbf{\Lambda}_i \mathbf{\Lambda}_i^H) \leq P_{\text{tot}}, \quad (37f)$$

$$\forall \mathbf{H}_{i,j} \in \mathbb{S}_R, \forall \mathbf{H}_{E_i} \in \mathbb{S}_E, \quad (37g)$$

where the new utility g_i is defined by

$$g_i = 2 \log \det(\mathbf{F}_{R_i}) - \alpha_i + d_s + 2 \log \det(\mathbf{F}_{E-i}) - \gamma_i + N_E + 2 \log \det(\mathbf{F}_{E+i}) - \beta_i + d_a - \sum_{j \neq i} \omega_j \theta_{i,j}, \quad (38)$$

in which $\mathbf{F}_{R_i} = \mathbf{S}_{R_i}^{\frac{1}{2}}$, $\mathbf{F}_{E-i} = \mathbf{S}_{E-i}^{\frac{1}{2}}$, $\mathbf{F}_{E+i} = \mathbf{S}_{E+i}^{\frac{1}{2}}$, and

$$\mathbf{\Xi}_{R_i} = \mathbf{S}_{R_i} \mathbf{M}_{R_i}, \quad (39)$$

$$\mathbf{\Xi}_{E+i} = \mathbf{S}_{E+i} \mathbf{M}_{E_i}, \quad (40)$$

$$\mathbf{\Xi}_{E-i} = \mathbf{S}_{E-i} (\mathbf{Z}_{E_i} + \mathbf{N}_{E_i}), \quad (41)$$

$$\mathbf{\Xi}_{R_i,j} = \mathbf{\Pi}_j \mathbf{H}_{i,j} (\mathbf{Q}_i \mathbf{Q}_i^H + \mathbf{\Lambda}_i \mathbf{\Lambda}_i^H) \mathbf{H}_{i,j}^H. \quad (42)$$

Although the objective function in (37) is convex, the problem (37) is still intractable due to the semi-definite constraints (37b)-(37e). We further transform this optimization problem into a solvable form in the following.

Upon exploiting the trace properties

$$\text{tr}(\mathbf{A} \mathbf{A}^H) = \|\text{vec}(\mathbf{A})\|^2, \quad (43)$$

$$\text{vec}(\mathbf{A} \mathbf{B} \mathbf{C}) = (\mathbf{C}^T \otimes \mathbf{A}) \text{vec}(\mathbf{B}), \quad (44)$$

and neglecting higher-order uncertainty terms, the semi-definite constraint (37b) can be rewritten as

$$\text{tr}(\mathbf{\Xi}_{R_i}) = \|\bar{\mathbf{\Xi}}_{R_i} + \Delta \mathbf{\Xi}_{R_i}\|^2 \leq \alpha_i, \quad (45)$$

where

$$\bar{\mathbf{\Xi}}_{R_i} = \begin{bmatrix} \text{vec}(\mathbf{F}_{R_i} (\sqrt{\omega_M} \mathbf{U}_{R_i}^H \bar{\mathbf{H}}_{i,i} \mathbf{Q}_i - \mathbf{I})) \\ \text{vec}(\sqrt{\omega_M} \mathbf{F}_{R_i} \mathbf{U}_{R_i}^H \bar{\mathbf{H}}_{i,i} \mathbf{\Lambda}_i) \\ \text{vec}(\mathbf{F}_{R_i} \mathbf{\Upsilon}_i^{\frac{1}{2}}) \\ \sigma_{R_i} \text{vec}(\mathbf{F}_{R_i}) \end{bmatrix}, \quad (46)$$

$$\Delta \mathbf{\Xi}_{R_i} = \begin{bmatrix} \overbrace{\mathbf{Q}_i^T \otimes (\sqrt{\omega_M} \mathbf{F}_{R_i} \mathbf{U}_{R_i}^H)}^{\mathbf{J}_{R_i}} \\ \overbrace{\mathbf{\Lambda}_i^T \otimes (\sqrt{\omega_M} \mathbf{F}_{R_i} \mathbf{U}_{R_i}^H)}^{\mathbf{J}_{R_i}} \\ \mathbf{0} \\ \mathbf{0} \end{bmatrix} \text{vec}(\Delta \mathbf{H}_{i,i}). \quad (47)$$

To eliminate the uncertainty $\Delta \mathbf{\Xi}_{R_i}$, the Schur complement lemma [19] are applied to define a hermitian matrix Φ that satisfy:

$$\Phi = \begin{bmatrix} \alpha_i & (\bar{\mathbf{\Xi}}_{R_i} + \Delta \mathbf{\Xi}_{R_i})^H \\ \bar{\mathbf{\Xi}}_{R_i} + \Delta \mathbf{\Xi}_{R_i} & \mathbf{I} \end{bmatrix} \succeq \mathbf{0}. \quad (48)$$

Thus, we have

$$\begin{bmatrix} \alpha_i & \overline{\mathbf{E}}_{R_i}^H \\ \overline{\mathbf{E}}_{R_i} & \mathbf{I} \end{bmatrix} \succeq \begin{bmatrix} 0 & -\Delta \overline{\mathbf{E}}_{R_i}^H \\ -\Delta \overline{\mathbf{E}}_{R_i} & \mathbf{0} \end{bmatrix}. \quad (49)$$

Furthermore, in consideration of sign-definiteness lemma [20, Lemma 1], define matrices \mathbf{A} , then, (49) can be transformed as

$$\mathbf{A} \succeq \mathbf{P}^H \mathbf{X} \mathbf{Q} + \mathbf{Q}^H \mathbf{X}^H \mathbf{P}, \quad (50)$$

where

$$\mathbf{A} = \begin{bmatrix} \alpha_i & \overline{\mathbf{E}}_{R_i}^H \\ \overline{\mathbf{E}}_{R_i} & \mathbf{I} \end{bmatrix}, \quad (51)$$

$$\mathbf{P} = \begin{bmatrix} \mathbf{0}^H & \mathbf{J}_{R_i,i}^H \end{bmatrix}, \quad (52)$$

$$\mathbf{Q} = \begin{bmatrix} -1 & \mathbf{0} \end{bmatrix}, \quad (53)$$

$$\mathbf{X} = \text{vec}(\Delta \mathbf{H}_{i,i}). \quad (54)$$

According to the sign-definiteness lemma, (50) holds if and only if there exist nonnegative real numbers λ_{α_i} such that

$$\begin{bmatrix} \begin{bmatrix} \alpha_i - \lambda_{\alpha_i} & \overline{\mathbf{E}}_{R_i}^H \\ \overline{\mathbf{E}}_{R_i} & \mathbf{I} \end{bmatrix} & -\zeta_{R_i,i} \begin{bmatrix} \mathbf{0}^T \\ \mathbf{J}_{R_i,i} \end{bmatrix} \\ -\zeta_{R_i,i} \begin{bmatrix} \mathbf{0} & \mathbf{J}_{R_i,i}^H \end{bmatrix} & \lambda_{\alpha_i} \mathbf{I} \end{bmatrix} \succeq \mathbf{0}, \quad (55)$$

where

$$\mathbf{J}_{R_i,j} = \begin{bmatrix} \mathbf{Q}_i^T \otimes \mathbf{\Pi}_j \\ \mathbf{\Lambda}_i^T \otimes \mathbf{\Pi}_j \end{bmatrix}. \quad (56)$$

Until now, (37b) has been transformed into a linear matrix inequality (LMI) (55).

Similarly, in the presence of nonnegative real numbers λ_{β_i} , λ_{γ_i} and $\lambda_{\theta_{i,j}}$, the constraints (37c)-(37e) are rewritten as the following corresponding LMIs:

$$\begin{bmatrix} \begin{bmatrix} \beta_i - \lambda_{\beta_i} & \overline{\mathbf{E}}_{E_{+i}}^H \\ \overline{\mathbf{E}}_{E_{+i}} & \mathbf{I} \end{bmatrix} & -\zeta_{E_i} \begin{bmatrix} \mathbf{0}^T \\ \mathbf{J}_{E_{+i}} \end{bmatrix} \\ -\zeta_{E_i} \begin{bmatrix} \mathbf{0} & \mathbf{J}_{E_{+i}}^H \end{bmatrix} & \lambda_{\beta_i} \mathbf{I} \end{bmatrix} \succeq \mathbf{0}, \quad (57)$$

$$\begin{bmatrix} \begin{bmatrix} \gamma_i - \lambda_{\gamma_i} & \overline{\mathbf{E}}_{E_{-i}}^H \\ \overline{\mathbf{E}}_{E_{-i}} & \mathbf{I} \end{bmatrix} & -\zeta_{E_i} \begin{bmatrix} \mathbf{0}^T \\ \mathbf{J}_{E_{-i}} \end{bmatrix} \\ -\zeta_{E_i} \begin{bmatrix} \mathbf{0} & \mathbf{J}_{E_{-i}}^H \end{bmatrix} & \lambda_{\gamma_i} \mathbf{I} \end{bmatrix} \succeq \mathbf{0}, \quad (58)$$

$$\begin{bmatrix} \begin{bmatrix} \theta_{i,j} - \lambda_{\theta_{i,j}} & \overline{\mathbf{E}}_{R_{i,j}}^H \\ \overline{\mathbf{E}}_{R_{i,j}} & \mathbf{I} \end{bmatrix} & -\zeta_{R_{i,j}} \begin{bmatrix} \mathbf{0}^T \\ \mathbf{J}_{R_{i,j}} \end{bmatrix} \\ -\zeta_{R_{i,j}} \begin{bmatrix} \mathbf{0} & \mathbf{J}_{R_{i,j}}^H \end{bmatrix} & \lambda_{\theta_{i,j}} \mathbf{I} \end{bmatrix} \succeq \mathbf{0}, \quad (59)$$

in which

$$\overline{\mathbf{E}}_{E_{+i}} = \begin{bmatrix} \text{vec}(\mathbf{F}_{E_{+i}}(\sqrt{\omega_E} \mathbf{U}_{E_i}^H \overline{\mathbf{H}}_{E_i} \mathbf{\Lambda}_i - \mathbf{I})) \\ \frac{\sigma_{E_i}}{\sqrt{\omega_E}} \text{vec}(\mathbf{F}_{E_{+i}} \mathbf{U}_{E_i}^H) \end{bmatrix}, \quad (60)$$

$$\mathbf{J}_{E_{+i}} = \begin{bmatrix} \mathbf{\Lambda}_i^T \otimes (\sqrt{\omega_E} \mathbf{F}_{E_{+i}} \mathbf{U}_{E_i}^H) \\ \mathbf{0} \end{bmatrix}, \quad (61)$$

$$\overline{\mathbf{E}}_{E_{-i}} = \begin{bmatrix} \text{vec}(\mathbf{F}_{E_{-i}} \overline{\mathbf{H}}_{E_i} \mathbf{Q}_i) \\ \text{vec}(\mathbf{F}_{E_{-i}} \overline{\mathbf{H}}_{E_i} \mathbf{\Lambda}_i) \\ \sigma_{E_i} \text{vec}(\mathbf{F}_{E_{-i}}) \end{bmatrix}, \quad (62)$$

$$\mathbf{J}_{E_{-i}} = \begin{bmatrix} \mathbf{Q}_i^T \otimes \mathbf{F}_{E_{-i}} \\ \mathbf{\Lambda}_i^T \otimes \mathbf{F}_{E_{-i}} \\ \mathbf{0} \end{bmatrix}, \quad (63)$$

$$\overline{\mathbf{E}}_{R_{i,j}} = \begin{bmatrix} \text{vec}(\overline{\mathbf{H}}_{i,j} \mathbf{Q}_i) \\ \text{vec}(\overline{\mathbf{H}}_{i,j} \mathbf{\Lambda}_i) \end{bmatrix}. \quad (64)$$

As a result, the robust design of AN-aided secrecy precoding and decoding matrices at each TX_{*i*}-RX_{*i*} pair can be reformulated as

$$\mathcal{P}_4 : \max_{\mathbf{Q}_i, \mathbf{\Lambda}_i, \mathbf{U}_{R_i}, \mathbf{U}_{E_i}, \mathbf{F}_{R_i}, \mathbf{F}_{E_{+i}}, \mathbf{F}_{E_{-i}} \succeq \mathbf{0}, \alpha_i, \beta_i, \gamma_i, \theta_{i,j} > 0} g_i, \quad (65a)$$

$$\text{s.t. (55), (57) - (59), (37f)}. \quad (65b)$$

Algorithm 1: Proposed ADP algorithm based on WMMSE

Initialization: Give maximum number of iterations

L_{\max} and termination threshold ϵ ;

Each transmitter i , $i \in \{1, 2, \dots, K\}$, chooses feasible AN-aided secrecy precoding \mathbf{Q}_i and $\mathbf{\Lambda}_i$, interference price, and auxiliary variables \mathbf{F}_{R_i} , $\mathbf{F}_{E_{+i}}$, $\mathbf{F}_{E_{-i}}$ and \mathbf{U}_{E_i} ;

Set $l = 0$;

while $\Delta g_i \geq \epsilon$ and $l \leq L_{\max}$ **do**

1. **for** $i = 1 : K$ **do**

1) Solve \mathcal{P}_4 to update \mathbf{U}_{R_i} with other parameters fixed at receiver RX_{*i*};

2) Solve \mathcal{P}_4 to update \mathbf{F}_{R_i} for fixed \mathbf{U}_{R_i} found in the previous step at receiver RX_{*i*};

3) Solve \mathcal{P}_4 to update \mathbf{F}_{R_i} for fixed \mathbf{U}_{R_i} found in the previous step at receiver RX_{*i*};

4) Calculate interference price $\mathbf{\Pi}_i$ based on (24) at TX_{*i*} and then broadcast it through a beacon;

5) Fixing \mathbf{F}_{R_i} and \mathbf{U}_{R_i} found in the previous steps, TX_{*i*} updates its AN-aided secrecy precoding $\{\mathbf{Q}_i, \mathbf{\Lambda}_i\}$ by solving \mathcal{P}_4 ;

6) Solve \mathcal{P}_4 to update \mathbf{U}_{E_i} for fixed $\mathbf{\Lambda}_i$ found in the previous step at TX_{*i*};

7) Solve \mathcal{P}_4 to update \mathbf{F}_{E_i} for fixed \mathbf{U}_{E_i} found in the previous step at TX_{*i*};

end

2. $l = l + 1$;

end

Output: Output results \mathbf{Q}_i^* , $\mathbf{\Lambda}_i^*$, $\mathbf{U}_{R_i}^*$.

The semi-definite program (SDP) problem \mathcal{P}_4 remains non-convex since some of the optimization variables are coupled with each other by multiplications, e.g., \mathbf{F}_{R_i} , \mathbf{U}_{R_i} , \mathbf{Q}_i and $\mathbf{\Lambda}_i$ in (55), and similar observations are obtained from (57) and (59). Fixing some optimization variables can make \mathcal{P}_4 into a convex optimization problem. In other words, with proper manipulations, its sub-problems become convex, readily solvable with the alternating convex search (ACS) method [21]. Algorithm 1 summarizes this proposed algorithm for solving the nonlinear nonconvex problem \mathcal{P}_4 .

B. Convergence and Optimality Analysis

1) *Convergence Analysis:* The convergence of Algorithm 1 is guaranteed because the objective utility function is monotonously increasing at each iteration and is bounded by power constraint and the interference price constraint (37e). Specifically, we have

$$\begin{aligned}
g_i^{n+1} &= g\left(\mathbf{F}_{E-i}^{n+1}, \mathbf{F}_{E+i}^{n+1}, \mathbf{U}_{E_i}^{n+1}, \mathbf{Q}_i^{n+1}, \mathbf{\Lambda}_i^{n+1}, \mathbf{F}_{R_i}^{n+1}, \mathbf{U}_{R_i}^{n+1}\right) \\
&\geq g\left(\mathbf{F}_{E-i}^{n+1}, \mathbf{F}_{E+i}^{n+1}, \mathbf{U}_{E_i}^{n+1}, \mathbf{Q}_i^{n+1}, \mathbf{\Lambda}_i^{n+1}, \mathbf{F}_{R_i}^n, \mathbf{U}_{R_i}^n\right) \\
&\geq g\left(\mathbf{F}_{E-i}^{n+1}, \mathbf{F}_{E+i}^{n+1}, \mathbf{U}_{E_i}^{n+1}, \mathbf{Q}_i^n, \mathbf{\Lambda}_i^n, \mathbf{F}_{R_i}^n, \mathbf{U}_{R_i}^n\right) \\
&\geq g\left(\mathbf{F}_{E-i}^{n+1}, \mathbf{F}_{E+i}^n, \mathbf{U}_{E_i}^n, \mathbf{Q}_i^n, \mathbf{\Lambda}_i^n, \mathbf{F}_{R_i}^n, \mathbf{U}_{R_i}^n\right) \\
&\geq g\left(\mathbf{F}_{E-i}^n, \mathbf{F}_{E+i}^n, \mathbf{U}_{E_i}^n, \mathbf{Q}_i^n, \mathbf{\Lambda}_i^n, \mathbf{F}_{R_i}^n, \mathbf{U}_{R_i}^n\right) = g_i^n,
\end{aligned} \tag{66}$$

which indicates that the objective function of \mathcal{P}_4 is non-decreasing during the optimization process. The utility function of each TX-RX pair incorporates the penalty for interference caused to other transmitters, and the constraint (37e) limits the interference price. Therefore, when optimizing g_i at TX_{*i*}-RX_{*i*} pair, it can ensure that the utility function, g_{i+1} , of the TX_{*i+1*}-RX_{*i+1*} pair does not decline. Due to power constraints, the utility function of each TX-RX pair is upper-bounded to ensure convergence of Algorithm 1.

2) *Optimality Analysis:* The KKT optimality conditions of the problem \mathcal{P}_1 (22) can be expressed as

$$\frac{\partial C_{S_i}}{\partial \mathbf{Q}_i^*} + \sum_{j \neq i} \frac{\partial C_{S_j}}{\partial \mathbf{Q}_i^*} + \lambda_{\mathbf{Q}_i} = 2 \lambda_i \mathbf{Q}_i^*, \tag{67}$$

$$\frac{\partial C_{S_i}}{\partial \mathbf{\Lambda}_i^*} + \sum_{j \neq i} \frac{\partial C_{S_j}}{\partial \mathbf{\Lambda}_i^*} + \lambda_{\mathbf{\Lambda}_i} = 2 \lambda_i \mathbf{\Lambda}_i^*, \tag{68}$$

where $\lambda_i, \lambda_{\mathbf{Q}_i}, \lambda_{\mathbf{\Lambda}_i} \geq 0$ are Lagrange multipliers of (22b), $\mathbf{Q}_i \succeq \mathbf{0}$ and $\mathbf{\Lambda}_i \succeq \mathbf{0}$. On the other hand, fixing $\mathbf{\Pi}_j$ for $j \neq i$, the KKT optimality conditions of the problem \mathcal{P}_2 (25) can be formulated as

$$\frac{\partial C_{S_i}}{\partial \mathbf{Q}_i^*} - 2 \sum_{j \neq i} \mathbf{H}_{i,j}^H \mathbf{\Pi}_j \mathbf{H}_{i,j} \mathbf{Q}_i^* + \lambda_{\mathbf{Q}_i} = 2 \lambda_i \mathbf{Q}_i^*, \tag{69}$$

$$\frac{\partial C_{S_i}}{\partial \mathbf{\Lambda}_i^*} - 2 \sum_{j \neq i} \mathbf{H}_{i,j}^H \mathbf{\Pi}_j \mathbf{H}_{i,j} \mathbf{\Lambda}_i^* + \lambda_{\mathbf{\Lambda}_i} = 2 \lambda_i \mathbf{\Lambda}_i^*. \tag{70}$$

Substituting $\mathbf{\Pi}_j$ (24) into (69) and (70), it can be seen that the KKT conditions (67) and (68) of the problem \mathcal{P}_1 is the same as the KKT conditions (69) and (70) of the problem \mathcal{P}_2 . This means that a local optimum of the problem (22) is also a local optimum of the problem (25). Furthermore, employing the MMSE receiver, the problem \mathcal{P}_2 is equivalent to the problem \mathcal{P}_3 (37), as proved in [4]. Additionally, the proposed algorithm for solving the problem \mathcal{P}_4 (65) converges to at least a local optimum solution of the problem \mathcal{P}_3 , as shown in [20]. Thus, the proposed algorithm for the problem \mathcal{P}_4 converges to a local optimum of the problem \mathcal{P}_1 .

C. Complexity Analysis

The computational complexity of Algorithm 1 is mainly from solving the problem \mathcal{P}_4 , which can be solved using the interior-point method [33] implemented by the CVX toolbox usable in Matlab with a computational complexity of $\mathcal{O}\left(\log\left(\frac{1}{\epsilon}\right)n_{\text{tot}}^{3.5}\right)$, where n_{tot} is the total number of real-valued optimization variables and ϵ is a given solution accuracy. Thus, by adding up the total number of optimization variables in the proposed optimization, the computational complexity of Algorithm 1 is expressed as

$$\begin{aligned}
C_{\text{pro-ADP}} &= \mathcal{O}\left(K \log\left(\frac{1}{\epsilon}\right) \left(N_T(d_s + d_a) + d_s(N_R + d_s) \right. \right. \\
&\quad \left. \left. + 3N_E^2 + 6 + 2K - 2\right)^{3.5}\right). \tag{71}
\end{aligned}$$

The computational complexity of MT-MSE scheme [5] is mainly from matrices multiplication, matrices inversion and solving polynomial equation of high degree. It is expressed as $C_{\text{MT-MSE}}$, where the complexity $c_{\text{MT-MSE1}}, c_{\text{MT-MSE1}},$ and $c_{\text{MT-MSE3}}$ arises from matrix multiplication and matrix inversion while solving the high-degree polynomial equation results in the complexity $c_{\text{MT-MSE4}}$. I denotes the total number of iteration steps, while h represents the number of steps required to solve the polynomial equation in each iteration step. In comparison, when $18 < N_T, N_R < 38$ while keeping other parameters fixed, we can obtain that $C_{\text{MT-MSE}} > C_{\text{pro-ADP}}$. However, it shows disadvantage when N_E grows.

$$c_{\text{MT-MSE1}} = KN_R N_T d_s + N_R^3 \tag{72}$$

$$c_{\text{MT-MSE2}} = KN_E N_T d_s + N_E^3 \tag{73}$$

$$c_{\text{MT-MSE3}} = KN_T N_R d_s + N_T^3 \tag{74}$$

$$c_{\text{MT-MSE4}} = h(2N_T)^2 \log(2N_T) \log \log(2N_T) \tag{75}$$

$$C_{\text{MT-MSE}} = \mathcal{O}(IK(c_1 + c_2 + c_3 + c_4)) \tag{76}$$

Similarly, the computational complexity of AN-IA scheme [6] is expressed as $C_{\text{AN-IA}}$. When $N_T, N_R < 20$, we can obtain $C_{\text{AN-IA}} > C_{\text{pro-ADP}}$. Besides, there are constraints on the number of transmitter, receiver, and eavesdropper antennas in the AN-IA scheme [6, Eq. (9)]. Otherwise, a closed-form solution does not exist.

$$c_{\text{AN-IA1}} = d_s N_T N_R + d_s^2 \tag{77}$$

$$c_{\text{AN-IA2}} = K(N_T N_R d_a + N_T d_a) \tag{78}$$

$$c_{\text{AN-IA3}} = K(N_T N_R d_s + N_T d_s) \tag{79}$$

$$c_{\text{AN-IA4}} = I(d_s N_R^3 + d_a N_E^3) \tag{80}$$

$$c_{\text{AN-IA5}} = IK(N_R N_T d_s + N_E N_T d_s) \tag{81}$$

$$\begin{aligned}
C_{\text{AN-IA}} &= \mathcal{O}(c_{\text{AN-IA1}} + c_{\text{AN-IA2}} + c_{\text{AN-IA3}} \\
&\quad + c_{\text{AN-IA4}} + c_{\text{AN-IA5}}) \tag{82}
\end{aligned}$$

IV. SIMULATIONS AND DISCUSSIONS

We consider a multiuser MIMO-IC network with $K = 3$. Unless otherwise specifically stated, the default parameters of the simulated network are $N_T = N_R = 4, d_s = 2,$

$d_a = 1$,³ $N_E = 8$, $d_M = d_I = 10$ m, $d_E = 10$ m, $P_{\text{tot}} = 20$ dB, and the noise variances $\sigma_{R_i}^2 = \sigma_{E_i}^2 = -110$ dB [23]. For convenience, we denote $\zeta_{E_i} = \zeta_{R_{i,j}} = \zeta$. Numerical simulations are carried out to evaluate the performance of our proposed AN-aided secrecy precoding design. Specifically, the convergence of the proposed algorithm is first verified through simulations. Next, we compare our proposed algorithm with the MT-MSE algorithm [5] and the AN-IA algorithm [6] in the simulations under both perfect and imperfect CSI conditions. Then, the impact of the imperfect CSI and eavesdropper on the achievable average secrecy rate of the proposed algorithm is further investigated to evaluate the robustness of our scheme.

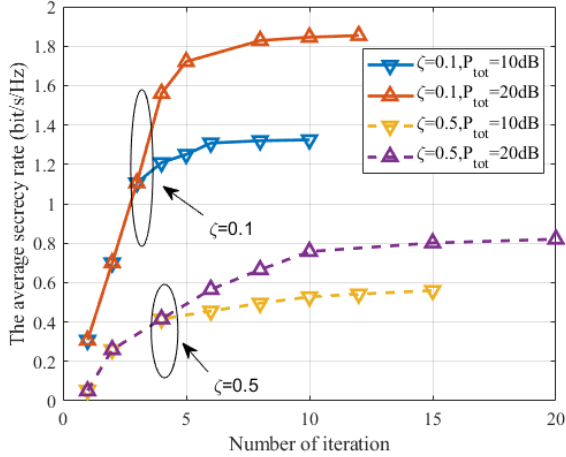


Fig. 3. Average secrecy rate versus number of iterations for Algorithm 1 under different transmitted power P_{tot} and CSI error bounds ζ , where $K = 3$, $N_T = N_R = 4$ and $N_E = 8$.

A. Convergence Performance of Proposed Algorithm

Fig. 3 investigates the convergence performance of Algorithm 1 by showing the average secrecy rate versus the number of iterations under different transmitted power and CSI error bounds ζ , where ζ is the squared root of the variance ζ^2 of the channel uncertainty defined in (13). It can be seen from Fig. 3 that Algorithm 1 achieves the fast convergence for all the four cases. As expected, the convergence speed and the attainable average secrecy rate depend on the CSI error bound ζ , and the total available transmit power P_{tot} .

Specifically, under the same P_{tot} , the smaller the CSI error bound, the faster the convergence, and the higher the achievable average secrecy rate. Observe that the influence of ζ on the convergence speed and the attainable average secrecy rate is particularly significant. In particular, Algorithm 1 converges within 10 iterations for $\zeta = 0.1$, and it converges within 15 iterations for $\zeta = 0.5$. Furthermore, given $P_{\text{tot}} = 10$ dB, the achievable average secrecy rates are 1.35 [bit/s/Hz] and 0.55 [bit/s/Hz] under $\zeta = 0.1$ and $\zeta = 0.5$, respectively, while given $P_{\text{tot}} = 20$ dB, the achievable average secrecy rates are 1.85 [bit/s/Hz] and 0.82 [bit/s/Hz] under $\zeta = 0.1$ and $\zeta = 0.5$, respectively. From both engineering and mathematical perspectives, when the CSI error bound is reduced, the feasible solution set of \mathcal{P}_4 is reduced, and Algorithm 1 can allocate

an optimal solution quicker, that is, the artificial noise can be more promptly and accurately aligned with the direction of the eavesdropper and secure precoding can also quickly find the optimal transmission direction. Increasing the CSI error bound has the opposite effect.

Similarly, the total available transmit power P_{tot} has some influence on the convergence speed. This is because as P_{tot} is reduced, the search space for the power constraints (37f) is shrunk, and hence the number of iterations required to achieve the optimal result decreases. Fig. 3 also shows that increased available transmit power improves the average secrecy rate. Although an increase in the transmitted power will simultaneously increase both the IUI and the strength of the confidential message signal at the legitimate receiver, as a benefit of the secure precoding based on interference management, the enhancement of the confidential message signal at the legitimate receiver will be more substantial than that of the IUI. Therefore, increasing the transmit power will improve the average secrecy rate.

B. Performance Comparison with Benchmarks

The comparison of the average secrecy rate of our scheme with those of the MT-MSE scheme [5] and the AN-IA scheme [6] is shown in Fig. 4 under both the perfect CSI case of $\zeta = 0$ and the imperfect CSI case of $\zeta = 0.1$, respectively, where Eve is equipped with $N_E = 8$ antennas. The AN-IA scheme [6] imposes stringent constraints on the number of antennas at the transmitter, receiver, and eavesdropper. Failure to meet these constraints results in the scheme's inability to determine a closed solution for variables during the iterative process. Moreover, both the AN-IA and MT-MSE schemes [5] necessitate a central node capable of accessing global channel information and executing iterative calculations, which is often impractical. In contrast, our proposed scheme is adaptable to any number of antennas at transmitters, receivers, and eavesdroppers. Unlike the conventional approach, where the achievable secrecy sum-rate of the system forms the objective function, our distributed scheme calculates the utility function independently for each TX-RX pair. Consequently, it is only essential for the i th TX-RX pair to access the CSI distribution (\mathbf{H}_{E_i} and $\mathbf{H}_{i,j}$) pertinent to it.

In the perfect CSI case with $\zeta = 0$, it can be seen that our proposed scheme outperforms the MT-MSE. This is because our scheme employs a direct and effective criterion that maximizes the utility function defined as the secrecy rate minus the interference cost imposed on other receivers⁴, instead of the MT-MSE criterion that minimizes the total MSE of the recovered signals. The MT-MSE criterion only approximates the direct security performance metric, i.e., the sum secrecy rate, thus resulting in some loss. It can also be seen that in the perfect CSI case, the performance gain of our scheme over the MT-MSE decreases with the increase of the transmit power. This is because the loss incurred by using the MT-MSE criterion decreases with the rise of the transmission power, as pointed out in [34]. It can also be seen

³Usually, one stream of IA is enough to degrade Eve [6]. Thus we set $d_a = 1$.

⁴This is fully equivalent to maximizing the sum secrecy rate, as proven in Subsection III-B.

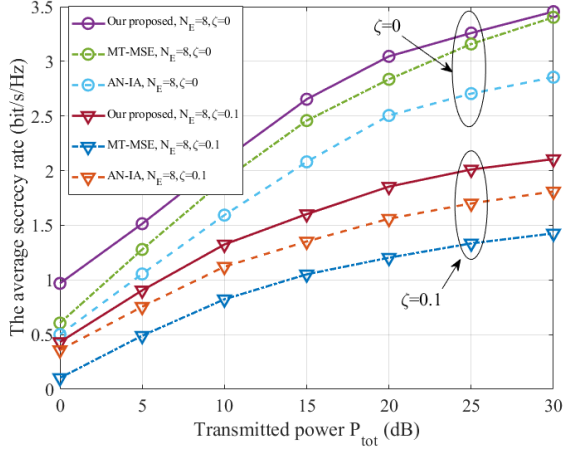


Fig. 4. Average secrecy rate versus available transmit power P_{tot} comparison of the proposed AN aided secrecy precoding scheme, MT-MSE scheme [5] and AN-IA scheme [6], where $K = 3$, $N_T = N_R = 4$ and $d_E = 10$ m.

that for the perfect CSI case, our scheme outperforms the AN-IA scheme considerably. The AN-IA scheme requires that the signal transmitted by each transmitter lies in the null space of the ICs at other non-paired receivers. However, when there is a strong correlation between the main channel and the IC, such constraints significantly reduce the communication rate of the main channel, thus decreasing the security rate.

In the imperfect CSI case with $\zeta = 0.1$, it is evident that our proposed scheme also outperforms both the MT-MSE and AN-IA. In particular, our scheme significantly outperforms the AN-IA scheme. Furthermore, unlike the perfect CSI case, the performance gain of our scheme over the MT-MS increases with the transmit power. This is indeed expected. The secrecy precoding in the MT-MSE scheme heavily relies on the perfect CSI of IC and EC to impose the IUI on Eve, not on the other legitimate receiver. Thus, with higher transmit power, the growth of the secrecy rate in the MT-MSE is more limited due to more leakage of IUI being injected into the legitimate receiver. By contrast, our method considers the CSI error bound of IC and EC, and enhancing the confidential message signal at the legitimate receiver is more substantial than that of the IUI with higher transmit power.

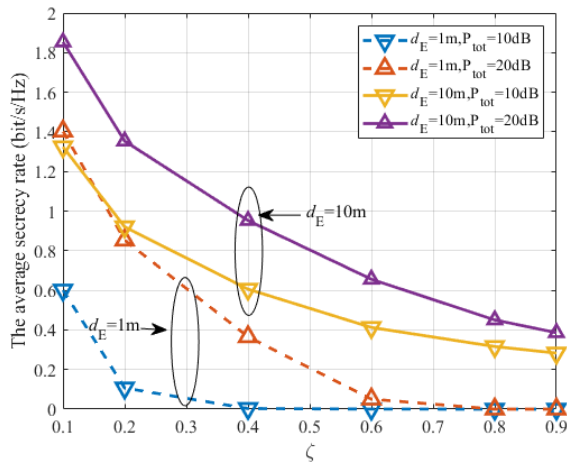


Fig. 5. Average secrecy rate versus CSI error bound ζ under two different positions of Eve, where $K = 3$, $N_T = N_R = 4$ and $N_E = 8$.

C. Impact of Imperfect CSI and Eavesdropper's Capability

We investigate the impact of imperfect CSI and eavesdropper's capability on our proposed scheme's achievable average secrecy rate.

First, Fig. 5 depicts our proposed scheme's achievable average secrecy rate as the function of the CSI error bound ζ under two different positions of Eve. As expected, the uncertainty in the main channel and ICs $\mathbf{H}_{i,j}$ as well as the EC \mathbf{H}_{E_i} has a significant impact on the achievable average secrecy rate. The average secrecy rate decreases significantly as the CSI error bound ζ increases. This is because a larger CSI error bound has a bigger negative impact on the secrecy precoding and the AN, which causes an increase in the IUI and leakage of confidential messages. As a result, the secrecy rate of each transmitter decreases. Furthermore, the distance between Eve and its targeted transmitter d_E greatly impacts the achievable average secrecy rate. Specifically, reducing d_E from 10 m to 1 m causes a significant drop in the average secrecy rate. This is because a smaller d_E than d_M makes the CSI of the EC better than that of the legitimate transceiver channel. Observe that in the case of $d_E = 1$ m with $P_{\text{tot}} = 10$ dB, the average secrecy rate is practically zero for $\zeta > 0.4$.

Not surprisingly, Eve's capability significantly impacts the achievable average secrecy rate. The ability of Eve depends on its number of antennas N_E and its distance to the targeted transmitter d_E . Fig. 6 portrays the impact of the eavesdropper's capability on the average secrecy rate of the proposed scheme. Specifically, when the number of Eve's antennas N_E increases, Eve can process signals from more spatial dimensions. Hence, its eavesdropping capability increases, and the average secrecy rate decreases. As the distance d_E between the transmitter and Eve decreases, Eve's channel gain increases. Hence, Eve's capability becomes stronger, and the security rate decreases. In addition, it can be seen from Fig. 6 that when d_E is very large, the influence of the number of Eve's antennas on the average secrecy rate decreases. This is because as d_E becomes large, the signal strength at the eavesdropper is

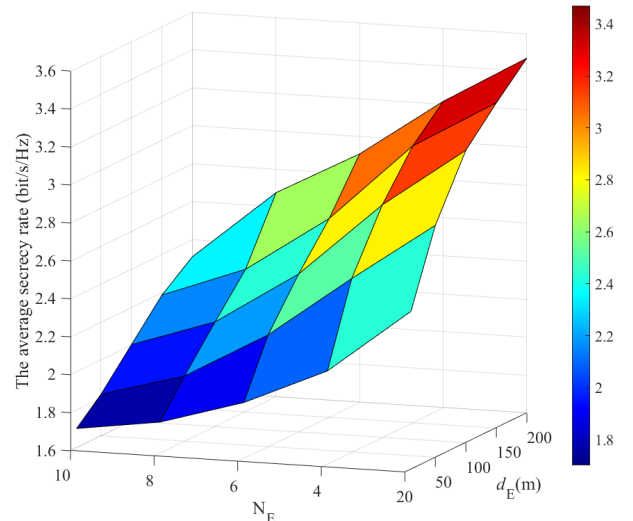


Fig. 6. Average secrecy rate versus Eve's number of antennas N_E and distance d_E , where $K = 3$, $\zeta = 0.1$, $d_E = (10, 50, 100, 150, 200)$ and $N_T = N_R = 4$.

reduced. Even if Eve can glean signals from more spatial dimensions, the total signal strength remains relatively low, and Eve's eavesdropping performance improvement remains relatively insignificant. Hence, the resultant reduction of the security rate remains relatively modest.

V. CONCLUSIONS

A distributed robust AN-aided secrecy precoding scheme has been proposed to secure communications over the wiretap MIMO-IC. Our scheme maximizes the sum secrecy rate by maximizing each user's utility while considering its interference cost imposed on the other users. Based on the ADP, WMMSE, Schur complement, and sign-definiteness techniques, the original non-convex optimization problem is transformed into a tractable approximate SDP problem subject to LMI constraints. This approximation problem is solved by the alternating convex search method. Our simulation study has demonstrated the efficiency of the proposed scheme. Specifically, the simulation results have confirmed the fast convergence of our proposed scheme. The results also show the superior performance of our scheme over the two well-known distributed secrecy precoding schemes for secure communications over the wiretap MIMO-IC.

REFERENCES

- [1] S. A. Jafar, *Interference Alignment – A New Look at Signal Dimensions in a Communication Network*. Hanover, MA, USA: now Publishers Inc. In: Found. Trends Commun. Inf. Theory, vol. 7, no. 1, pp. 1-130, 2010.
- [2] Z. Sheng, H. D. Tuan, A. A. Nasir, H. V. Poor, and E. Dutkiewicz, "Physical layer security aided wireless interference networks in the presence of strong eavesdropper channels," *IEEE Trans. Inf. Forensics Secur.*, vol. 16, pp. 3228–3240, May 2021.
- [3] V. R. Cadambe and S. A. Jafar, "Interference alignment and degrees of freedom of the K -user interference channel," *IEEE Trans. Inf. Theory*, vol. 54, no. 8, pp. 3425–3441, Aug. 2008.
- [4] A. Abrardo, G. Fodor, and M. Moretti, "Distributed digital and hybrid beamforming schemes with MMSE-SIC receivers for the MIMO interference channel," *IEEE Trans. Veh. Technol.*, vol. 68, no. 7, pp. 6790–6804, Jul. 2019.
- [5] Z. Kong, *et al.*, "Iterative distributed minimum total MSE approach for secure communications in MIMO interference channels," *IEEE Trans. Inf. Forensics Secur.*, vol. 11, no. 3, pp. 594–608, Mar. 2016.
- [6] N. Zhao, F. R. Yu, M. Li, and V. C. M. Leung, "Anti-eavesdropping schemes for interference alignment (IA)-based wireless networks," *IEEE Trans. Wirel. Commun.*, vol. 15, no. 8, pp. 5719–5732, Aug. 2016.
- [7] D.-H. Chen, Y.-C. He, X. Lin, and R. Zhao, "Both worst-case and chance-constrained robust secure SWIPT in MISO interference channels," *IEEE Trans. Inf. Forensics Secur.*, vol. 13, no. 2, pp. 306–317, Feb. 2018.
- [8] J. Huang, R. A. Berry, and M. L. Honig, "Distributed interference compensation for wireless networks," *IEEE J. Sel. Areas Commun.*, vol. 24, no. 5, pp. 1074–1084, May 2006.
- [9] L. Hu, S. Tan, H. Wen, J. Wu, J. Fan, S. Chen, and J. Tang, "Interference alignment for physical layer security in multi-user networks with passive eavesdroppers," *IEEE Trans. Inf. Forensics Secur.*, vol. 18, pp. 3692–3705, Jun. 2023.
- [10] S. Jia, *et al.*, "Secure multiantenna transmission with an unknown eavesdropper: Power allocation and secrecy outage analysis," *IEEE Trans. Inf. Forensics Secur.*, vol. 17, pp. 2906–2919, Aug. 2022.
- [11] A. M. Alaa and M. H. Ismail, "Achievable degrees of freedom of the K -user SISO interference channel with blind interference alignment using staggered antenna switching," *IEEE Trans. Veh. Technol.*, vol. 66, no. 3, pp. 2825–2829, Mar. 2017.
- [12] O. El Ayach, S. W. Peters, and R. W. Heath, "The practical challenges of interference alignment," *IEEE Wirel. Commun.*, vol. 20, no. 1, pp. 35–42, Feb. 2013.
- [13] L. Tian, W. Liu, Y. Geng, J. Li, and T. Q. S. Quek, "Wireless distributed computing networks with interference alignment and neutralization," *IEEE Trans. Commun.*, vol. 72, no. 2, pp. 740–755, Feb. 2024.
- [14] A. Ghasemi, A. S. Motahari, and A. K. Khandani, "Interference alignment for the K -user MIMO interference channel," *IEEE Trans. Inf. Theory*, vol. 68, no. 3, pp. 1401–1411, Mar. 2022.
- [15] N. Zhao, *et al.*, "Interference alignment and its applications: A survey, research issues, and challenges," *IEEE Commun. Surv. Tutor.*, vol. 18, no. 3, pp. 1779–1803, Third Quarter 2016.
- [16] D. Yang, J. Xu, W. Xu, B. Sheng, X. You, C. Yuen, and M. Di Renzo, "Spatially correlated RIS-aided secure massive MIMO under CSI and hardware imperfections," *IEEE Trans. Wirel. Commun.*, vol. 23, no. 9, pp. 11461–11475, Sep. 2024.
- [17] C. Jiang, C. Zhang, C. Huang, J. Ge, J. He and C. Yuen, "Secure beamforming design for RIS-assisted integrated sensing and communication systems," *IEEE Wirel. Commun. Lett.*, vol. 13, no. 2, pp. 520–524, Feb. 2024.
- [18] Q. Shi, M. Razaviyayn, Z.-Q. Luo, and C. He, "An iteratively weighted MMSE approach to distributed sum-utility maximization for a MIMO interfering broadcast channel," *IEEE Trans. Signal Process.*, vol. 59, no. 9, pp. 4331–4340, Sep. 2011.
- [19] R. A. Horn and C. R. Johnson, *Matrix Analysis*. Cambridge, U.K.: Cambridge University Press, 1985.
- [20] E. A. Gharavol and E. G. Larsson, "The sign-definiteness lemma and its applications to robust transceiver optimization for multiuser MIMO systems," *IEEE Trans. Signal Process.*, vol. 61, no. 2, pp. 238–252, Jan. 2013.
- [21] J. Gorski, F. Pfeuffer, and K. Klamroth, "Biconvex sets and optimization with biconvex functions—A survey and extensions," *Mathematical Methods of Operations Research*, vol. 66, no. 3, pp. 373–408, Dec. 2007.
- [22] A. Samir, *et al.*, "Performance of NOMA-based dual-hop hybrid powerline-wireless communication systems," *IEEE Trans. Veh. Technol.*, vol. 71, no. 6, pp. 6548–6558, Jun. 2022.
- [23] N. Zhao, *et al.*, "Secure transmission for interference networks: User selection and transceiver design," *IEEE Systems Journal*, vol. 13, no. 3, pp. 2839–2850, Sep. 2019.
- [24] H. Jia, X. Li, and L. Ma, "Physical layer security optimization with Cramér–Rao bound metric in ISAC systems under sensing-specific imperfect CSI model," *IEEE Trans. Veh. Technol.*, vol. 73, no. 5, pp.6980–6992, May 2024.
- [25] J. B. Perazzone, P. L. Yu, B. M. Sadler, and R. S. Blum, "Artificial noise-aided MIMO physical layer authentication with imperfect CSI," *IEEE Trans. Inf. Forensics Secur.*, vol. 16, pp. 2173–2185, Feb. 2021.
- [26] Z. Zhai, W. Lei, H. Lei, and H. Tang, "Robust design of the security scheme in IRS-assisted MISO systems with imperfect eavesdropping CSI," *IEEE Trans. Veh. Technol.*, vol. 73, no. 9, pp. 12815–12827, Sep. 2024.
- [27] S. Atapattu, *et al.*, "Physical-layer security in full-duplex multi-hop multi-user wireless network with relay selection," *IEEE Trans. Wirel. Commun.*, vol. 18, no. 2, pp. 1216–1232, Feb. 2019.
- [28] N. Su, *et al.*, "Physical layer security for multi-user MIMO visible light communication systems with generalized space shift keying," *IEEE Trans. Commun.*, vol. 69, no. 4, pp. 2585–2598, Apr. 2021.
- [29] Y. Jiang and Y. Zou, "Secrecy energy efficiency maximization for multi-user multi-eavesdropper cell-free massive MIMO networks," *IEEE Trans. Veh. Technol.*, vol. 72, no. 5, pp. 6009–6022, May 2023.
- [30] A. ElSamadouny, A. El Shafie, M. Abdallah, and N. Al-Dhahir, "Secure sum-rate-optimal MIMO multicasting over medium-voltage NB-PLC networks," *IEEE Trans. Smart Grid*, vol. 9, no. 4, pp. 2954–2963, Jul. 2018.
- [31] X. Cao and K. J. R. Liu, "Distributed Newton's method for network cost minimization," *IEEE Trans. Autom. Control.*, vol. 66, no. 3, pp. 1278–1285, Mar. 2021.
- [32] Y. Ge and J. Fan, "Robust secure beamforming for intelligent reflecting surface assisted full-duplex MISO systems," *IEEE Trans. Inf. Forensics Secur.*, vol. 17, pp. 253–264, Jan. 2022.
- [33] S. Boyd and L. Vandenberghe, *Convex Optimization*. New York, USA: Cambridge University Press, 2004.
- [34] T. Koike-Akino, *et al.*, "Capacity, MSE and secrecy analysis of linear block precoding for distributed antenna systems in multi-user frequency-selective fading channels," *IEEE Trans. Commun.*, vol. 59, no. 3, pp. 888–900, Mar. 2011.



Zhengmin Kong (Senior Member, IEEE) received the B.Eng. and Ph.D. degrees from the School of Electronic Information and Communications, Huazhong University of Science and Technology, Wuhan, China, in 2003 and 2011, respectively. From 2005 to 2011, he was a member of the Research Staff with the Wuhan National Laboratory for Optoelectronics, where he was involved in beyond-3G and UWB system design. From 2014 to 2015, he was an Academic Visitor with the University of Southampton, Southampton, U.K., where he investigated physical layer security and artificial intelligence. He is currently an Associate Professor with the School of Electrical Engineering and Automation, Wuhan University. His current research interests include physical layer security, signal processing, power information technology and artificial intelligence, in particular physical layer security and interference management.

He is currently an Associate Professor with the School of Electrical Engineering and Automation, Wuhan University. His current research interests include physical layer security, signal processing, power information technology and artificial intelligence, in particular physical layer security and interference management.



Jing Song received the B.Eng. and M.S. degrees from the School of Electrical and Automation, Wuhan University, Wuhan, China, in 2019 and 2022 respectively. She has been working in Kunming Power Supply Bureau since 2022. Her current research interests include power line communication and signal processing, interference management schemes in MIMO interference channels, capacity analysis in multiuser communication systems, and physical layer security.

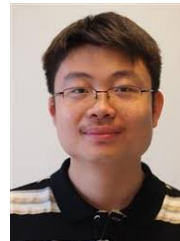


Shaoshi Yang (Senior Member, IEEE) received the B.Eng. degree in information engineering from Beijing University of Posts and Telecommunications (BUPT), China, in 2006, and the Ph.D. degree in electronics and electrical engineering from University of Southampton, U.K., in 2013. From 2008 to 2009, he was a Researcher with Intel Labs China. From 2013 to 2016, he was a Research Fellow with the School of Electronics and Computer Science, University of Southampton. From 2016 to 2018, he was a Principal Engineer with Huawei Technologies

Co., Ltd., where he made significant contributions to the products, solutions and standardization of 5G, wideband IoT, and cloud gaming/VR. He was a Guest Researcher with the Isaac Newton Institute for Mathematical Sciences, University of Cambridge. He is currently a Full Professor with BUPT, and a Deputy Director of the Key Laboratory of Mathematics and Information Networks, Ministry of Education, China. His research interests include 5G/5G-A/6G, massive MIMO, mobile ad hoc networks, distributed artificial intelligence, and cloud gaming/VR. He is a standing committee member of the CCF Technical Committee on Distributed Computing and Systems. He received Dean's Award for Early Career Research Excellence from University of Southampton in 2015, Huawei President Award for Wireless Innovations in 2018, IEEE TCGCC Best Journal Paper Award in 2019, IEEE Communications Society Best Survey Paper Award in 2020, CAI Invention and Entrepreneurship Award in 2023, CIUR Industry-University-Research Institute Cooperation and Innovation Award in 2023, and the First Prize of Beijing Municipal Science and Technology Advancement Award in 2023. He is an Editor of *IEEE Transactions on Communications*, *IEEE Transactions on Vehicular Technology*, and *Signal Processing* (Elsevier). He was also an Editor for *IEEE Systems Journal* and *IEEE Wireless Communications Letters*. For more details of his research progress, please refer to <https://shaoshiyang.weebly.com/>.



Li Gan received the B.S. degree in automation from Wuhan University, Wuhan, China, in 2022, where she is currently pursuing the M.S. degree with the School of Electrical Engineering and Automation. Her research interests include wireless communications and signal processing, power line communication and OFDM, capacity analysis in multiuser communication systems, and physical layer security.



Weizhi Meng (Senior Member, IEEE) is a Full Professor in the School of Computing and Communications, Lancaster University, U.K., and an adjunct faculty in the Department of Applied Mathematics and Computer Science, Technical University of Denmark, Denmark. He obtained his Ph.D. degree in Computer Science from the City University of Hong Kong. He was a recipient of the Hong Kong Institution of Engineers (HKIE) Outstanding Paper Award for Young Engineers/Researchers in both 2014 and 2017. He also received the IEEE ComSoc Best

Young Researcher Award for Europe, Middle East, Africa Region (EMEA) in 2020 and the IEEE ComSoc Communications Information Security (CISTC) Early Career Award in 2023. His primary research interests are blockchain technology, cyber security and artificial intelligence in security, including intrusion detection, blockchain applications, smartphone security, biometric authentication, and IoT security.



Tao Huang (Senior Member, IEEE) received his Ph.D. degree in electrical engineering from The University of New South Wales, Australia, in 2016. He received the M.Eng. degree in sensor system signal processing from The University of Adelaide, Australia, in 2007 and the B.Eng. degree in electronics and information engineering from Huazhong University of Science and Technology, China, in 2003. Dr. Huang is a Senior Lecturer at James Cook University (JCU), Cairns, Australia. He is the Head of the International Partnerships in the College of

Science and Engineering and the Intelligent Computing and Communications Lab Director at JCU. He was an Endeavour Australia Cheung Kong Research Fellow, a Visiting Scholar at The Chinese University of Hong Kong, a Research Associate at the University of New South Wales, and a Postdoctoral Research Fellow at James Cook University. Before joining academia, Dr. Huang was a Senior Engineer, Senior Data Scientist, Project Team Lead, and Technical Lead in industry. Dr. Huang has received the Best Paper Award from IEEE WCNC in 2011, the IEEE Outstanding Leadership Award in 2022, and the IEEE Access Outstanding Associate Editor Award in 2023. He is a co-inventor of an international patent on MIMO systems. Dr. Huang is the Vice Chair of the IEEE Northern Australia Section and the local MTT-S/ComSoc Chapter Chair. He is an Associate Editor of *IEEE Open Journal of Communications Society*, *IEEE Access*, and *IET Communications*. His research interests include deep learning, intelligent sensing, computer vision, pattern recognition, wireless communications, system optimization, electronics systems, and IoT security.



Sheng Chen (Life Fellow, IEEE) received his B.Eng. degree from the East China Petroleum Institute, Dongying, China, in 1982, and his Ph.D. degree from The City University, London, in 1986, both in control engineering. He was awarded the higher doctoral degree, Doctor of Sciences (D.Sc.), from University of Southampton, Southampton, U.K., in 2005. From 1986 to 1999, he held research and academic appointments at The University of Sheffield, The University of Edinburgh, and University of Portsmouth, all in U.K. Since 1999, he has been with

the School of Electronics and Computer Science, University of Southampton, U.K., where he holds the post of Professor in Intelligent Systems and Signal Processing. Dr. Chen's research interests include adaptive signal processing, wireless communications, modeling and identification of nonlinear systems, neural network and machine learning, evolutionary computation methods and optimization. He has published over 700 research papers. Dr. Chen has 20,000+ Web of Science citations with h-index 62 and 39,000+ Google Scholar citations with h-index 84. Dr. Chen is a Fellow of the Royal Academy of Engineering, U.K., a Fellow of Asia-Pacific Artificial Intelligence Association (AAIA), and a Fellow of IET. He is one of the original ISI highly cited researchers in engineering (March 2004).